Flow Turbulence Combust
DOI 10.1007/s10494-015-9626-0

Mixing Modelling Framework Based on Multiple Mapping Conditioning for the Prediction of Turbulent Flame Extinction

K. Vogiatzaki[1] · S. Navarro-Martinez[2] · S. De[3] · A. Kronenburg[3]

Received: 5 January 2015 / Accepted: 6 June 2015

Abstract A stochastic implementation of the Multiple Mapping Conditioning (MMC) approach has been applied to a turbulent piloted jet diffusion flame (Sandia flame F) that is close to extinction. Two classic mixing models (Curl's and IEM) are introduced in the MMC context to model the turbulent mixing. The suggested model involves the use of a reference space (that is mapped to mixture fraction space) in order to define particle proximity. The addition of the MMC ideas to the IEM and Curl's models, that is suggested in the current work, aspires to combine the simplicity of these two models with the enforced compositional locality without violating the linearity and independence principles. The formulation of the approach is discussed in detail and results are presented for the mixing field and reactive species. The predictions are compared with joint-scalar PDF simulations using the same mixing models and experimental data. Moreover, the sensitivity of the model to the particle number is examined. It is shown that MMC is less sensitive to the number of particles and can generally produce improved predictions of major and minor chemically reacting species with a lower number of particles.

✉ K. Vogiatzaki
konstantina.vogiatzaki.2@city.ac.uk

S. Navarro-Martinez
s.navarro@imperial.ac.uk

S. De
santanu.de@itv.uni-stuttgart.de

A. Kronenburg
kronenburg@itv.uni-stuttgart.de

[1] School of Engineering and Mathematical Sciences, City University, EC1V 0HB, London, UK

[2] Mechanical Engineering Department, Imperial College London, SW7 2AZ, London, UK

[3] Institut für Technische Verbrennung, University of Stuttgart, 70569, Stuttgart, Germany

JrnlID 10494_ArtID 9626_Proof#1 - 19/06/2015

Keywords Multiple mapping conditioning · Mixing models · Probability density function approach · Sandia flame F

1 Introduction

An important safety issue for engineers of combustion systems is the appearance of local extinction and re-ignition of the flame. These phenomena can be directly linked to the levels of turbulence in the combustion chamber. Overall, turbulence is a physical process highly desirable in combustion devices since it enhances the mixing of the fuel and oxidiser and accelerates the combustion process. However, due to its chaotic nature, small changes can result in a considerable increase of its intensity. If a critical value is exceeded very small eddies are generated that can penetrate the reaction zone reducing the flame temperature and disrupting the formation of radicals. Under these conditions the chemistry deviates from equilibrium and regions on the stoichiometric surface begin to extinguish. This could lead to global flame extinction or the flame may re-ignite depending on local strain-rate conditions.

Direct Numerical Simulation (DNS) would be the only numerical method capable of providing a detailed description of extinction and re-ignition since burning and mixing occurs mostly at the smallest scales. However, due to the very large computing requirements Large-eddy (LES) and Reynolds averaged (RANS) simulations are the two alternative methods commonly used that involve some extra modelling. Although LES has drawn considerable attention of the academic community over the last decade, its application has not yet quite reached the industry sector. On the other hand RANS based CFD codes are still widely used in industries. In both, the RANS and LES contexts the instantaneous scalar dissipation –the term used to describe the levels of the mixing rate– is unclosed and thus the research around new turbulence combustion approaches that represent more accurately the mixing process is still very important.

The objective of the present work is to ascertain the capability of the Multiple Mapping Conditioning (MMC) approach [21] and its closures to capture local extinction and re-ignition in laboratory flames in the RANS context. The MMC framework combines the probability density function (PDF) approach [27] and the mixture fraction based methods [20] via the application of a generalised mapping function to a prescribed reference space. PDF methods have been extensively applied to the modelling of turbulent reacting flows and a relatively recent comprehensive review is given by Haworth [14]. Of particular relevance are the studies by Pope and co-workers [3, 4, 36] where sensitivities of the PDF modelling approach towards parameters such as the mixing model [4], the mixing time scale [4] and the chemical mechanism [3] were investigated. Raman and Pitsch [30] successfully adapted the PDF methods as sub-grid scale model for large-eddy simulations. The Sandia flame series with flames of moderate to significant local flame extinction (Sandia Flames E and F) [1, 2] served as a test bed for all these modelling validation studies, and the same flames are used here for the validation of the MMC models.

With respect to the MMC modelling, stochastic and deterministic formulations exist, and both formulations have been explored in the past for the simple case of Sandia flame D [32, 33], a flame with a relatively low degree of extinction. Variants of the original MMC formulation have been successfully applied to Sandia Flame E (and Flame F) using a hybdrid binomial Langevin-MMC model for the modelling of the velocity-scalar interactions [35] or using a sparse particle method as sub-grid model for LES of the turbulent flow and mixing fields [12, 13]. In this work we focus exclusively on the stochastic implementation in the

JrnlID 10494_ArtID 9626_Proof#1 - 19/06/2015

RANS context, we base the MMC mixing model on the IEM and Curl's models (as opposed to IEM only that was used in earlier work [33]), we expand our study to the more challenging case of Sandia flame F, a flame with a relatively high Reynolds number and a considerable degree of extinction and re-ignition that has never been explored in the MMC context, and we assess the model dependence on the number of particles used for the stochastic solution of the composition field.

2 Turbulence-Chemistry Interaction Model

2.1 The PDF approach

Conventional PDF methods are based on the solution of the following equation that describes the evolution of the joint (one point) scalar PDF $P = P(y, \mathbf{x}, t)$ of a set of n_s scalars Y_I $(I = 1, .., n_s)$.

$$\frac{\partial \langle\rho\rangle P_Y}{\partial t} + \nabla(\langle\rho\rangle u_Y P_Y) + \frac{\partial \langle\rho\rangle \langle\Omega|y\rangle P_Y}{\partial y_i} + \frac{\partial^2 \langle\rho\rangle N_{IJ} P_Y}{\partial y_i \partial y_j} = 0, \tag{1}$$

where u_Y is the conditional expectation of the flow velocity v $(u_Y(y, \mathbf{x}, t) = \langle \mathrm{v}|Y = y\rangle)$ and N_{IJ} is the conditional scalar dissipation, $N_{IJ} = \langle D\nabla Y_I \nabla Y_J|Y = y\rangle$, which is by definition symmetric and positive semidefinite. The term D is the diffusion coefficient D_{IJ} (which is assumed to be the same for all species in high Reynolds number flows) and Ω_I is the reaction rate.

The most commonly adopted approach to solving the above PDF evolution equation is the Lagrangian stochastic particle method, where the evolution of an ensemble of particles is used to represent the evolution of the (Eulerian) joint PDF of Eq. 1. In terms of implementation of the framework, a Lagrangian solver for the composition joint PDF is coupled with a standard Eulerian approach [14, 24, 25]. The solution domain in physical space is discretized into a number of cells for the purpose of extracting local mean quantities such as velocities which are then used in the particle evolution equations. Then, moments of reactive species, temperature and mixture fraction can be extracted by ensemble (or weighted) average of the particles in the same Eulerian cell. Properties of particles drawn from the same cell are considered to be local in the physical space. This approach is followed in the current work as well. Equation 1 is replaced by an equivalent set of stochastic differential equations of the following form

$$dx^* = (\mathrm{v}(\mathrm{x}^*, \mathrm{t}) + \frac{1}{\rho}\frac{\partial}{\partial \mathrm{x}}(\rho(\mathrm{D} + \mathrm{D_t})))\mathrm{dt} + \sqrt{2(\mathrm{D} + \mathrm{D_t})}\mathrm{dw_i^*}, \tag{2}$$

$$dY_I^* = [\Omega_I^* + S_I^*]dt. \tag{3}$$

The underlying idea is that the Fokker-Planck equation [11] that corresponds to the above set of equations has the same moments as those given by the PDF transport Eq. 1. Here and for the remainder of the paper, the superscript '*' is used to distinguish the values linked to stochastic trajectories (stochastic particles), from deterministic quantities, D_t is the turbulent diffusivity and approximated by $D_t \approx 0.09 * k^2/\epsilon/\sigma_t$ with $\sigma_t = 0.7$ being the turbulent Schmidt number. Equation 2 accounts for transport in physical space while Eq. 3 accounts for transport in the composition space. The location of the particles is indicated as x^*, w_i^* is a Wiener process with zero mean and variance equal to dt and S^* is a mixing operator that simulates the rate of change of scalar dissipation and in the Lagrangian particle context it represents (in a stochastically equivalent sense) the composition change of a fluid

JrnlID 10494_ArtID 9626_Proof#1 - 19/06/2015

particle under the effect of molecular mixing. The $v(x^*, t)$ term is calculated by using the mean Eulerian velocity field $v(x, t)$ interpolated to the particle position x^*.

For the modelling of S^* certain principles should be satisfied by the mixing models such as boundedness of the scalars, linearity of scalar transport, independence of the evolution of the particle properties and most importantly localness in the physical and compositional spaces [27, 31]. Treating fluid as continuum, molecular diffusion is an exchange of composition between neighboring fluid particles which are infinitesimally close in both position and in composition. Although localness in the physical space is easy to impose in most models by allowing "mixing" among particles that belong to the same cell, localness in composition space is a major problem and much more difficult to impose [26]. Results [31] suggest that if particles mix with other particles in their immediate neighbourhood in composition space so that mixing across the reaction zone is avoided, the description of mixing is improved. On the contrary "artificial" extinction can be predicted for turbulent non-premixed flames at infinite Damköler number if the principle of localness in composition space is violated. An additional difficulty is that in reality localness in the physical space and localness in the composition space in particle methods are two principles that interlink. In a recent study by [19] it is demonstrated that closeness in physical space can be related –in addition to localness in composition space– to the number of particles used in the calculations and of course to the resolution limitations originating from the resolution of the underlying Eulerian flow fields.

Different models have been suggested in the literature for S^*. Simple models that are easy to implement, such as the interaction by exchange with the mean (IEM) [10] and the various Curl's models [9, 16] do not ensure localness in the composition space. A more recent model, the Euclidean minimum spanning tree (EMST) [31] enforces locality but implementation is rather complicated, and it violates the linearity and independence principles. A promising new model the shadow-position mixing model (SPMM), was introduced in 2013 in [29] however up to date its applicability has only been demonstrated for the idealised case of a reactive scalar mixing layer. The addition of the MMC ideas to the IEM and Curl's model that is suggested in the current work and described in detail in the next section, aspires to combine the simplicity of these two models with the enforced compositional locality without violating the linearity and independence principles.

2.2 The MMC concept

MMC, by the use of a reference space, addresses some of the problems described in the previous section associated with the modelling of the mixing term. The basic idea of the mapping closure concept [5, 28] is to employ turbulent fluctuations and small-scale mixing in a mathematical reference space, ξ, with a known (or prescribed) PDF to model the mixing in the physical composition space with unknown PDF. A deterministic implementation of the method leads to closure of the conditional scalar dissipation [7, 17]. In the present paper, we focus on a stochastic implementation. If the reference space is chosen properly it can be used to enforce localness in composition space [21, 34]. The idea is to track particle position in the reference space and then allow mixing only among particles that are close to each other in ξ-space. Theoretically, events close in physical space should also be close in composition space, ensuring the localness of the MMC model.

The suggested approach can considered to be an extension to the work of Wandel et al. [34] and has already been applied for the case of Sandia flame D using IEM as the only underlying mixing model [33]. It is a probabilistic MMC formulation with a single reference variable that is used to enforce localness in mixture fraction space and whose evolution

JrnlID 10494_ArtID 9626_Proof#1 - 19/06/2015

is described by a Markov process. MMC allows the choice of any number of reference variables, yet for flames with low levels of local extinction, localness in mixture fraction space is known to be sufficient to indicate localness in the multidimensional composition space. In a broader sense the shadow position model of [29] can be seen as a variation of the MMC concept where instead of enforcing locality through mixture fraction space, mixing is modeled as a relaxation of the composition to its mean conditional on the shadow position. In the present work we test if the enforced locality imposed by MMC can capture the behaviour of flames close to blow off.

We introduce a stochastic reference variable, ξ^*, which is governed by the following set of sdes

$$dx^* = U(\xi^*)dt, \tag{4}$$

$$d\xi^* = A^o dt + b^o dw^* \tag{5}$$

and for which we assume that the distribution is known.

The Fokker-Planck equation representing the above sde can be written as

$$\frac{\partial P_\xi}{\partial t} + \nabla \mathbf{U} P_\xi + \frac{\partial A^o P_\xi}{\partial \xi} - \frac{\partial^2 B^o P_\xi}{\partial \xi^2} = 0, \tag{6}$$

where $2B^o = (b^o)^2$. Considering an arbitrary function of ξ^*, $f(\xi^*) = f^*$ a corresponding sde for this new random variable can be generated using an Ito transformation:

$$df(\xi^*) = \widetilde{A}dt + \widetilde{b}dw^*, \tag{7}$$

with

$$\widetilde{A} = \frac{\partial f(\xi)}{\partial t} + U\nabla f(\xi) + \left(A^o \frac{\partial f(\xi)}{\partial \xi} + B^o \frac{\partial^2 f(\xi)}{\partial \xi^2} \right) \tag{8}$$

and

$$\widetilde{b} = b^o \frac{\partial f(\xi)}{\partial \xi} \tag{9}$$

The Fokker Planck equation representing the above sde is given by

$$\frac{\partial P_f}{\partial t} + \nabla U P_f + \frac{\partial \widetilde{A} P_f}{\partial f} - \frac{\partial^2 \widetilde{B} P_f}{\partial f^2} = 0. \tag{10}$$

The advantage of the "mapping " is that by assuming a shape for P_ξ we can define A^o and b^o from Eq. 6. We can then define the unknown drift and diffusion coefficients for the new stochastic process $f(\xi^*)$ and consequently the evolution of its PDF. It should be noted that the equivalent PDF describes the one-point one-time cell distribution. A two-point strategy has been suggested based on mapping functions that incorporate two-points statistics [15] however it has not been attempted here.

Following the probabilistic approach and adding to the equations for a standard PDF approach, Eqs. 2 and 3, the two new MMC equations, Eqs. 5 and 7, that embody the mapping closure concept, the general probabilistic approach gives

$$dx^* = U(\xi^*)dt, \tag{11}$$

$$d\xi^* = A^o dt + b^o dw^*, \tag{12}$$

$$d\overline{Y}(\xi^*) = \widetilde{A}dt + \widetilde{b}dw^*, \tag{13}$$

$$dY^* = [\Omega_I^* + S_I^*]dt. \tag{14}$$

It should be noticed that Eq. 13 is not solved since it is in reality equivalent to Eq. 12. This mathematical equivalence is the key that explaines the concept that an appropriate choice of the reference space will also guarantee localness in composition space. To keep

the computational cost low, the reference variables generate the fluctuations of a selected number of species only (the so called "major species") and the fluctuations of the remaining species (the so called "minor species") are linked to the fluctuations of major species similar to the conditional moment closure methodology [21]. Thus, it is only necessary to establish mapping relations as Eq. 13 for the major species and this is here mixture fraction, Z. For each major species that has a corresponding reference variable, the MMC transport equation becomes a PDF transport equation [21], [18]. Thus, A^o, B^o and $U(\xi^*)$ must be chosen so that $\widetilde{A}$ and $\widetilde{B}$ describe a diffusion process for mixture fraction. If we assume a Gaussian distribution for the reference variable and equate Eqs. 10 to 1 for mixture fraction we can obtain the unknown coefficient A^o and b^o from

$$\mathbf{U} = \mathbf{U}(\xi; \mathbf{x}, t) = \mathbf{U}^{(0)} + \mathbf{U}^{(1)}\xi, \tag{15}$$

$$A^o = -\frac{\partial B^o}{\partial \xi} + B^o\xi + \frac{1}{\langle\rho\rangle}\nabla\langle\rho\rangle\mathbf{U}^{(1)} + \frac{2}{P_\xi}\frac{\partial B^o P_\xi}{\partial \xi}, \tag{16}$$

$$\mathbf{U}^{(0)} = \langle \mathrm{v} \rangle, \tag{17}$$

$$\mathbf{U}^{(1)}\langle \xi Z \rangle = \langle \mathrm{v}^{'}\mathrm{Z}^{'} \rangle. \tag{18}$$

The turbulent flux can be modelled by a standard gradient approximation, $\langle \mathrm{v}^{'}\mathrm{Z}^{'} \rangle = -\mathrm{D_t}\nabla < \mathrm{Z} >$ and $\langle \xi Z \rangle$ results directly from the solution of $Z(\xi)$ (c.f Fig. 1). The term B^o is modelled independently of ξ, $B^o = B^o(\mathbf{x}, t)$), and is related to the scalar dissipation $\langle N_Z \rangle$ through

$$B^o \left\langle \left(\frac{\partial Z}{\partial \xi} \right)^2 \right\rangle = \langle N_Z \rangle. \tag{19}$$

It is apparent from Eq. 19 that closure of the MMC model requires knowledge of the unconditional scalar dissipation of Z, but it does not explicitly include the more difficult to model conditional scalar dissipation. The dissipation $\langle N_Z \rangle$ can be modelled adopting Corrsin's suggestion [8] that the decay rate of a passive scalar variance is assumed to be proportional to the decay rate of the turbulent kinetic energy i.e.

$$\langle N_Z \rangle = 0.5\frac{\langle Z^{'2} \rangle}{\tau_D}, \tag{20}$$

where τ_D is proportional to the flow turbulent time scale $\tau = k/\varepsilon$ with a proportionality constant commonly assumed to be $C_D = 1/C_\phi = 0.5$.

It should be noted that three different definitions of fluctuations exist in MMC: the unconditional fluctuations or major fluctuations $Y_I' = Y_I - \langle Y_I \rangle$, the minor fluctuations $Y_I'' = Y_I - \langle Y_I|\xi \rangle$ and the fluctuations around a quantity, conditionally averaged on mixture fraction itself, $Y_I''' = Y_I - \langle Y_I|Z \rangle$. The diffusion coefficient B^o controls the major fluctuations while the mixing operator S_I^* controls the minor fluctuations. In the current work two different models have been implemented which are essentially modified versions of the well known IEM and Curl's model.

When using the modified IEM model (MMC-IEM) the particles are mixed with their means conditioned on a certain value in the reference space $\langle Y_I|\xi \rangle$

$$S_I^* = \frac{1}{2}\frac{\overline{Y_I}(\xi^*) - Y_I^{*p}}{\tau_{min}}. \tag{21}$$

For the modified version of the Curl's model (MMC-Curl's) at each time step all particles that belong to the same Eulerian cell are formed into pairs and mix with their mean. The selection of every particle pair is not random as in commonly used Curl's models but it is

JrnlID 10494_ArtID 9626_Proof#1 - 19/06/2015

according to the distance of the particles in the reference space. For the present work, only particles that belong to the same ξ-bin are allowed to mix following

$$S_I^* = \frac{1}{2}\frac{0.5(Y_I^{*p} + Y_I^{*q}) - Y_I^{*p}}{\tau_{min}}, \tag{22}$$

with $< S^*|\xi^*, x^* >= 0$ [21]. The simplicity of both models is attractive for implementation, but the estimation of the "minor dissipation time", τ_{min}, is rather problematic since minor fluctuations exist only in the context of MMC. Wandel and Klimenko [34] used DNS of homogeneous turbulence to obtain a time scale ratio between the minor and major dissipation time of $\tau_{min}/\tau_D = 1/8$. However, Vogiatzaki et al. [33] could not corroborate these findings for laboratory jet diffusion flames. Mixing time scales smaller than τ_D were found to suppress most minor fluctuations and lead to a significant underprediction of the conditionally averaged variances. For Sandia Flame D, best results were obtained with $\tau_{min} = \tau_D$, and this value is adopted here.

3 Computational Methods

The test case (Sandia flame F) [1] consists of a methane/air fuel mixture that issues from a central d= 7.2mm internal diameter nozzle surrounded by a coaxial pilot flame with an outer diameter of 18.2mm. The fuel is 25 % CH_4 and 75 % air by volume with a stoichiometric mixture fraction of $Z_{st} = 0.351$. The jet Reynolds number is 44,800, the pilot inlet velocity is $22.8m/s$ and the velocity of the co-flowing air is $0.9m/s$.

The PDF approach is used in order to model the turbulence-chemistry interaction. The composition PDFs are calculated by Monte Carlo methods, while a finite-volume method was applied to solve for the mean velocity, dissipation, and mean pressure fields. The Eulerian flow field equations are solved using an in-house RANS code (BOFFIN). Turbulence is modelled by a standard k-ε model [23]. A cylindrical domain extends $0.65m$ in downstream direction and $0.15m$ in radial direction and is discretised by 200 axial and 100 radial finite volume cells. An augmented reduced mechanism (ARM2) derived from the full GRI 3.0 mechanism using quasi-steady assumptions for some minor species is incorporated to describe the chemical reactions [6]. Cao and Pope [3] demonstrated that ARM2 is capable of predicting the correct extinction levels for all Sandia Flames D-F but for flame F, results may be sensitive towards small changes in the boundary conditions or modelling parameters. For the composition field calculations, three different particle densities have been used in order to asses the sensitivity of the models on particle number. The different test cases are listed in Table 1. The evolution of the particle properties is modelled by Eqs. 11 to 14. We emphasise that every particle carries information on its (stochastic) velocity, species concentration, temperature *and* reference space ξ, obtained from Eq. 12.

Note that the reference space is Gaussian and unbounded, but the deterministic drift term counteracts the random diffusion term and keeps particles close to the mean. Then

Table 1 Overview of the test cases with corresponding number of particles

Test case	Number of Particles	Particles per cell
1	400.000	20
2	1.000.000	50
3	2.000.000	100

JrnlID 10494_ArtID 9626_Proof#1 - 19/06/2015

depending on their ξ value the particles within each cell are ordered in the reference sample space that extends from -4 to 4, divided into 16 ξ-bins. In each ξ-bin, $\langle Y_I|\xi\rangle$ is defined by an ordinary averaging process. For empty ξ-bins, values are obtained from linear interpolation.

It is important to emphasize that the calculations with 20 particles/cell take 5 hours on a single core machine. The computational cost is tripled when the number of particles is increased to 100 particles per cell. Previous Lagrangian PDF approaches in the RANS context use a wide range of particle numbers (from 100 particles/cell [36] to 800 particles/cell [24]). Although the absolute computational time depends on the specific characteristic of the codes used in these calculations, it is obvious that a significant increase of the number of particles will significantly increase the computational cost. This increase can be very important for the calculation of a realistic industrial geometry with a considerably bigger grid. Thus, a very desirable characteristic of any new mixing model is to perform well with a relatively low number of particles per cells. This motivated the three numerical experiments with different numbers of particles

4 Results and Discussion

Figure 1 is a graphic representation of the MMC concept at x/d =15 at three radial locations of the flame under consideration: on the rich side (r/d = 0.1), in the shear layer (r/d =1) and on the lean side (r/d = 2). As mentioned above every particle carries a set of values that represent its (stochastic) velocity, species concentration, temperature *and* ξ. This creates a correlation between temperature, (or any reactive species), mixture fraction and reference

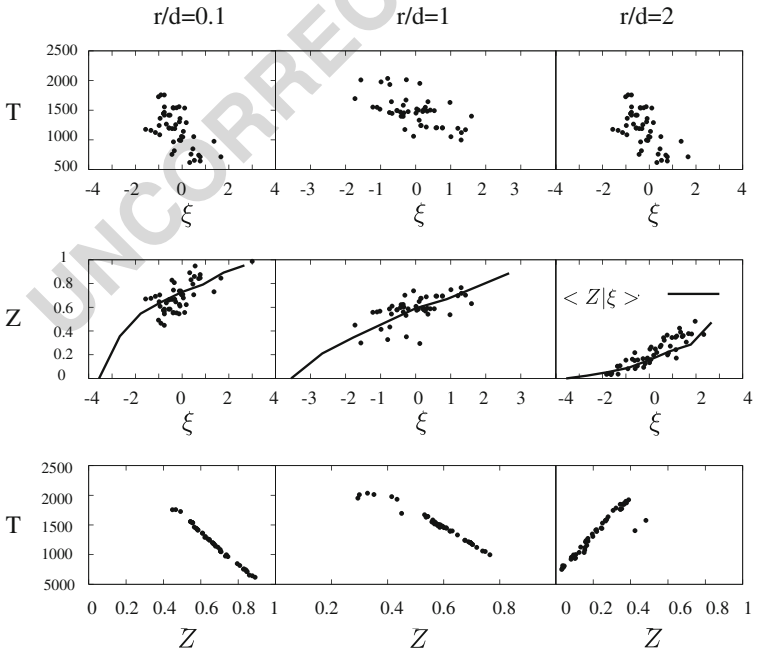

Fig. 1 MMC mapping concept: *first row* – temperature versus reference space at three radial locations; *second row* – computed mapping function; *third row* – temperature versus mixture fraction for the MMC-IEM mixing model

JrnlID 10494_ArtID 9626_Proof#1 - 19/06/2015

space which is demonstrated in the top two rows of the figure. Closeness of the particles in the reference space controls closeness of the particles in the mixture fraction fraction space and consequently in the temperature (or composition) space as can be seen in the figures in the bottom row. This correlation exists only because the evolution of the reference space, Eq. 12, is not independent of the evolution of the species, Eq. 13. Consequently, mixing particles that are close in reference space is equivalent to mixing particles close in composition space. It is important to stress that if the particle's value of the reference space was held constant throughout the calculations, the reference variable and mixture fraction would decorrelate with time (or distance from the jet exit) and the method would collapse to a conventional PDF approach. The decorrelation would be equivalent to horizontal lines of the averaged mixture fraction, $\langle Z \mid \xi \rangle$, in the middle row of Fig. 1.

In Fig. 2 the radial profiles of the mean and root mean square (rms) of the mapping function (mixture fraction) are presented for all four mixing models, IEM, MMC-IEM, Curl's and MMC-Curl's. It is apparent that the mixing field is quite insensitive to the choice of the mixing model. The simulations presented in this figure are performed with 20 particles/cell, the quality of predictions for test cases 1 to 3 (see Table 1) is comparable for all models and none of them shows a significant dependence on the particle number. As it has been shown in previous studies [4, 36] the predictions for the mixture fraction depend mostly on the choice of the mixing time scale that for the current work is the same for all four models.

Figures 3, 4, 5 and 6 show the scatter plots of temperature at different axial locations for three different particle loadings. Figure 7 shows the experimental results and serves as comparison. These figures allow a qualitative assessment, and MMC (both with IEM and Curl's), yields a somewhat more realistic scatter in temperature with fewer realizations above equilibrium conditions than the classic models. The MMC-IEM model is not capable of fully capturing the extent of extinguished flame elements as seen in the experiments, but it needs to be emphasized here that MMC-IEM provides qualitatively reasonable predictions even with a very small number of particles. These results should be compared with

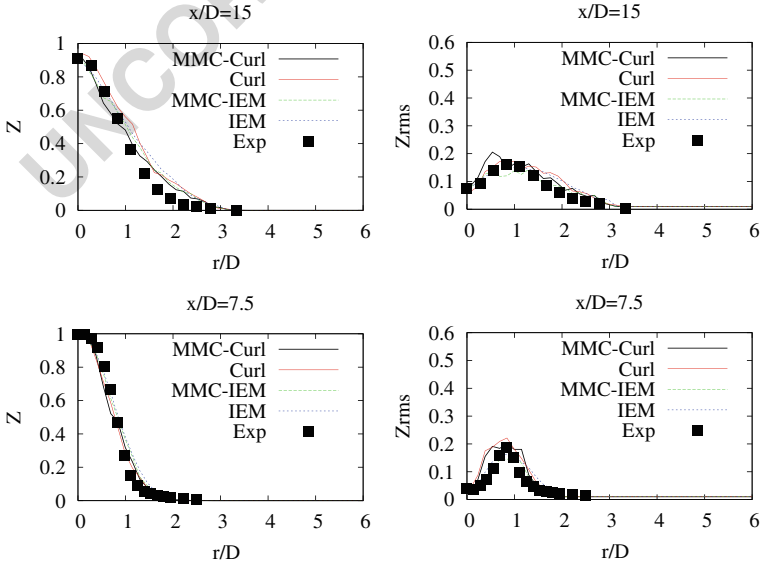

Fig. 2 Radial profiles of mean (*left*) and rms (*right*) of mixture fraction Z at different axial locations

JrnlID 10494_ArtID 9626_Proof#1 - 19/06/2015

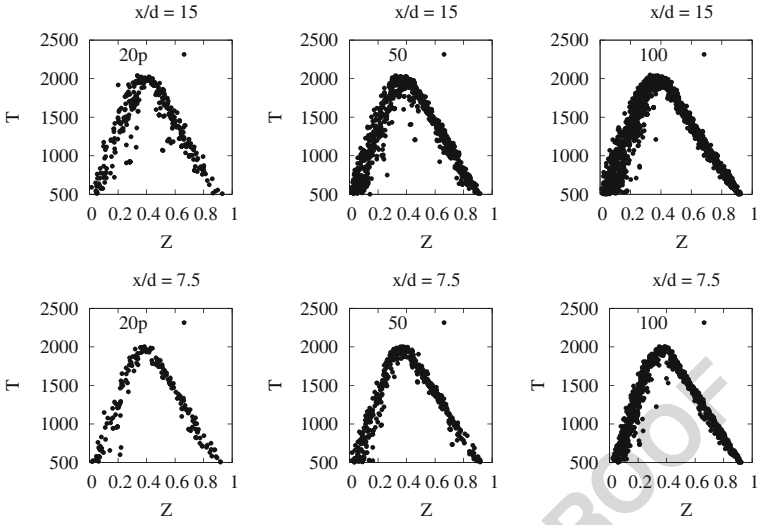

Fig. 3 MMC-IEM: scatter plots of temperature at different axial locations and for different particle number densities

306 conventional IEM simulations (see Fig. 4). The IEM mixing model creates two very dis-
307 tinct branches, one burning and one non-burning, that are not present in Fig. 7 and yield an
308 unphysical bias towards certain realizations in composition space. Note that the computa-
309 tion of the mean value in the cell, used for the mixing model, is based on the instantaneous
310 cell population and it slightly varies with the iteration and is thus dependent on the number

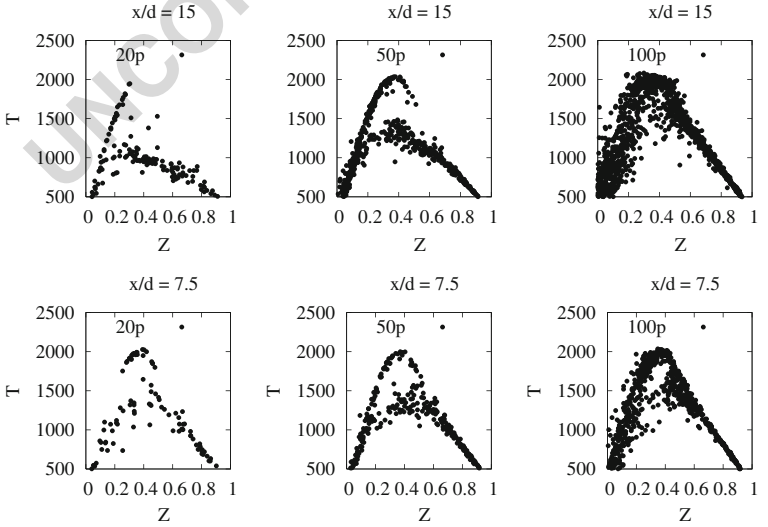

Fig. 4 IEM: Scatter plots of temperature at different axial locations and for different particle number densities

JrnlID 10494_ArtID 9626_Proof#1 - 19/06/2015

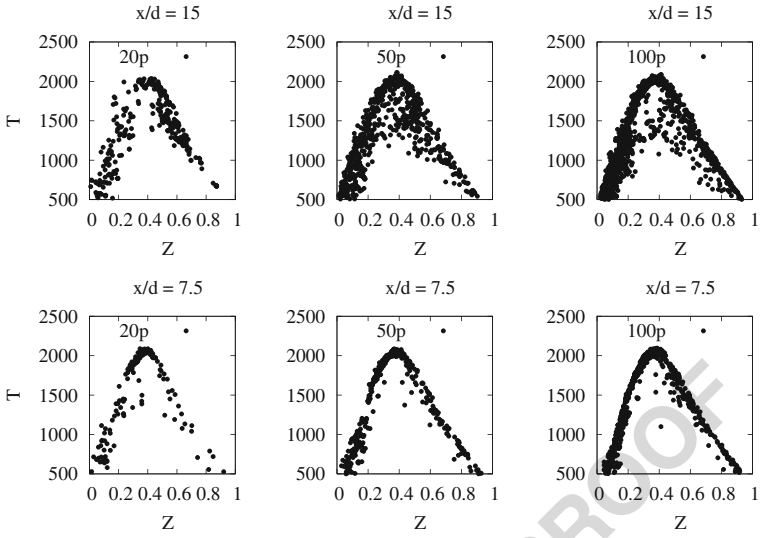

Fig. 5 MMC-Curl's: Scatter plots of temperature at different axial locations and for different particle number densities

of the particles in the cell. The dependence of the IEM model on particle number would vanish if averages over many iteration would be used instead.

The MMC-Curl's model appears to provide the best qualitative agreement with the experimental data especially further downstream. The conventional Curl's model also predicts the extinction satisfactorily, but some spurious behaviour can be observed especially on the lean side when only few particles are used. The reader should note that we have used the

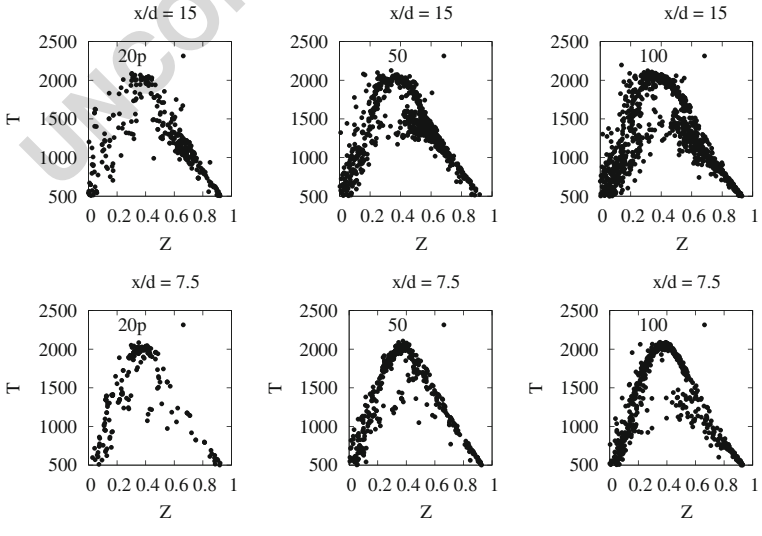

Fig. 6 Curl's: Scatter plots of temperature at different axial locations and for different particle number densities

JrnlID 10494_ArtID 9626_Proof#1 - 19/06/2015

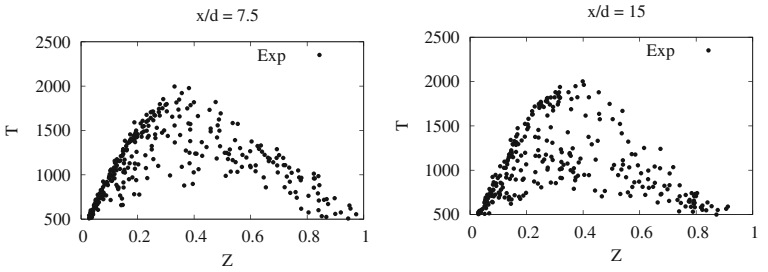

Fig. 7 Experiment: Scatter plots of temperature at different axial locations

simple Curl's model in its original form and not its modified version. No additional control of the mixing process to limit unphysical super-equilibrium values has been attempted.

A better insight is provided by Figs. 8 and 9. Here, the radial profiles of the conditional temperature and its conditional rms at different axial locations are presented and the MMC-IEM and IEM models can be compared. It can be clearly seen that IEM shows a strong dependence on the particle number while MMC-IEM is much less sensitive to particle density and only 20 particles per cell yield an independence of the solution from the particle density while IEM requires around 100 particles/cell to approximate the same results. The conditional rms are considerably under-predicted for the MMC-IEM and the IEM model appears to be somewhat better. However these predictions should be always viewed in conjunction with Figs. 3 and 4. The high rms values result from unphysical mixing of particles that create two distinct burning modes rather than a uniform scattering as the one seen in the experiments (see Fig. 7).

These trends are similar but much less pronounced for MMC-Curl's and Curl's model (not shown here). MMC-Curl's and Curl's yield conditional temperatures closer to the experimental values at both axial locations, and the classic Curl's mixing model is only

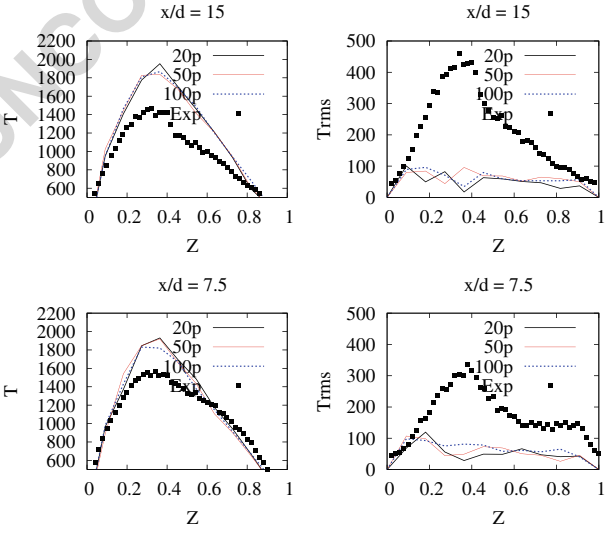

Fig. 8 Radial profiles of conditional temperature and rms at different axial locations with MMC-IEM

JrnlID 10494_ArtID 9626_Proof#1 - 19/06/2015

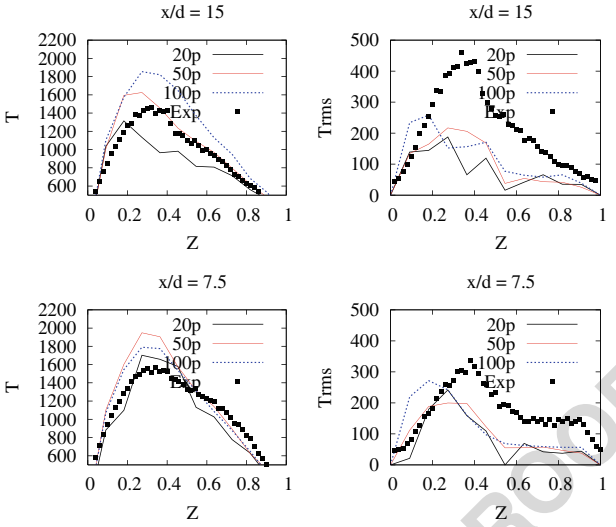

Fig. 9 Radial profiles of conditional temperature and rms at different axial locations with IEM

slightly more sensitive to the particle number density than MMC-Curl's. The better agreement with experimental data can be attributed to the fact that pair-wise models are known to model mixing more realistically than mean based models. It is emphasized again, that for all test cases the same mixing constant has been used, and no efforts have been made to control mixing through the mixing time scale as is a common practice. This does not necessarily imply that all the models have the best performance with the same constant. Adjustments of the mixing constant C_ϕ could have led to more realistic degrees of extinction and can have effects on the stability of the numerical solution but may deteriorate the mixing field predictions [4] and would not aid the analysis of the differences between MMC-*enhanced* mixing models and the particle number dependence.

The predictions of the radial profiles of temperature (not shown here) are generally less sensitive to the number of particles for all models and the same holds for species such as CH_4. It can be noticed that for all the test cases the temperature predictions are satisfying and a small improvement is noticed with the addition of MMC for radial positions r/d > 1.5 (towards the lean side of the flame). On the other hand the prediction of species such as CO or H_2O that are more sensitive to small changes of temperature is more challenging and more dependent on the quality of the mixing model. Figures 10 and 11 show the radial profiles of CO at different axial locations. MMC shows less sensitivity to the particle number when compared to IEM and less noise than Curl's, which indicates increased numerical stability that was reported to be an issue in earlier PDF calculations when using IEM and Curl's mixing models [4, 36]. MMC-Curl's with 100 particles/cell gives the overall best agreement.

IEM and MMC-IEM have opposite tendency when the particle number is increased at x/d=15; the more particles are used in IEM, the higher the temperature, re-igniting the flame. This is consistent with the scatter plot in Fig. 4 where the lower branch disappears as the number of particles increases. MMC-IEM have a much more uniform behaviour, with minimum difference in temperature predictions with particle refinement. Doubling the number of particles barely decreases the peak temperature by 50 K. The particle dependence of IEM

JrnlID 10494_ArtID 9626_Proof#1 - 19/06/2015

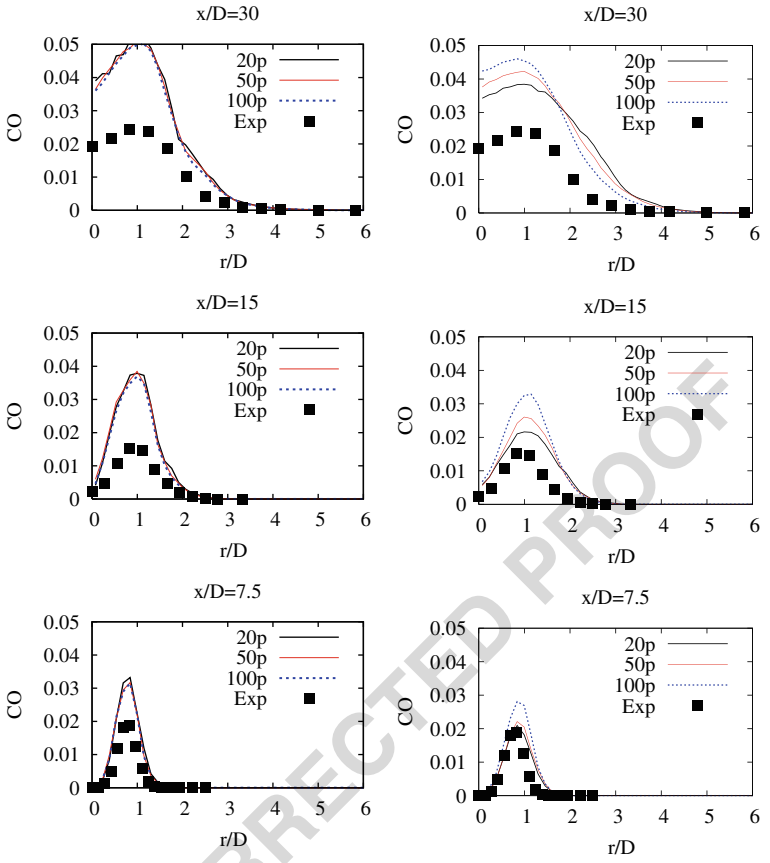

Fig. 10 Radial profiles of CO at different axial locations with MMC-IEM (*left*) IEM(*right*)

is amplified, when we look at CO predictions (see Fig. 10) at x/d=15. At the same position the MMC-IEM shows no particle number dependency, although it under-predicts extinction as observed in Fig. 8.

When the Curl's mixing sub-model is used, both MMC-Curl's and Curl's exhibit large particle dependency in and around the zone with significant extinction (see Fig. 11). This suggests that when extinction occurs, large numbers of particles per cell are indeed needed. However, away from it, fewer particles per cell are needed in the MMC context as the extra dependence on the reference space improves the mixing description. Probably more than one reference space is needed when severe extinction occurs, a modification suggested in previous studies as well [7, 22]. In the case of Curl's, large fluctuations are observed even with 100 particles per cell, while MMC produces smoother statistics. This can be easily understood by the nature of the corresponding SDE's of the MMC and PDF methods, Eqs. 13 and 2, respectively. The diffusion coefficient of MMC equations can be zero locally, unlike the PDF equations, and therefore statistical noise can be globally reduced.

An additional observation is that MMC shows better behaviour along the centreline and this is probably due to a better numerical treatment of the conditional velocity close to the centreline. It is not in the scope of this paper to explore the modelling of the conditional

JrnlID 10494_ArtID 9626_Proof#1 - 19/06/2015

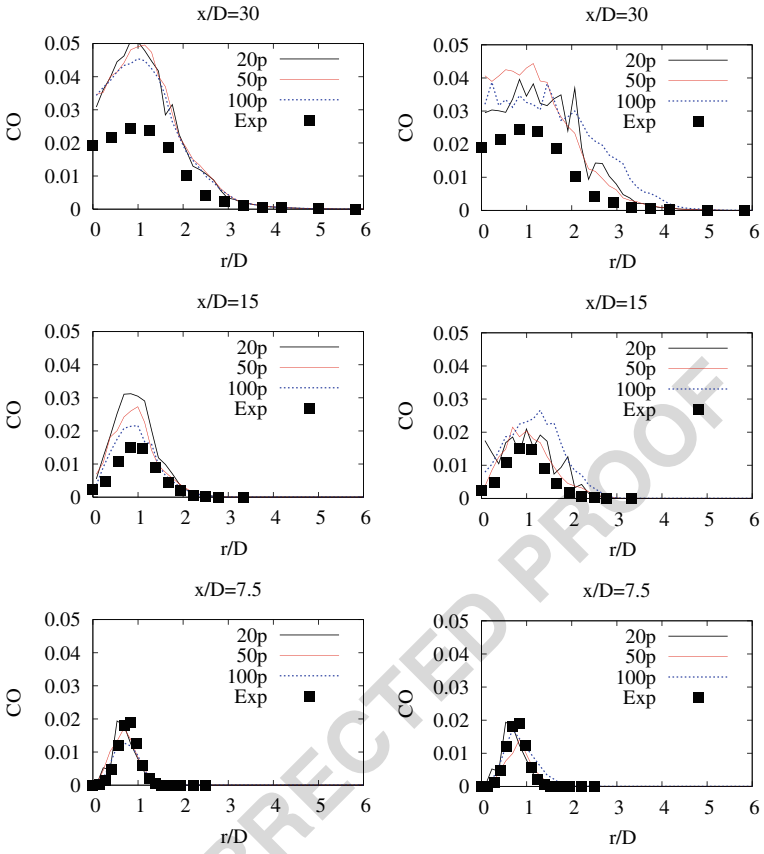

Fig. 11 Radial profiles of CO at different axial locations with MMC-Curl's (*left*) Curl's (*right*)

velocity, however, it can be briefly noticed from Eq. 15 and 18 that the fluctuating part of the velocity becomes zero when the gradients of mixture fraction are zero allowing particles to follow the mean flow field trajectories.

5 Conclusion

In this paper we suggest a numerical framework for modelling the mixing term of the joint-scalar PDF. Two models are tested for the prediction of the degree of extinction of a piloted non-premixed turbulent methane flame close to blow off. The behaviour of two new mixing models has been assessed in the MMC context and compared to common mixing models in the literature. The models suggested in this work are extensions of two classic mixing models (Curl's and IEM) and aspire to overcome the deficiencies of the classical models modelling of flames close to extinction. The results indicate that by introducing to the Curl's and IEM model indirect localness in the mixture fraction space through the use of the reference space, the predictions' sensitivity to the number of particles is reduced. This trend is more pronounced for the MMC-IEM variation of the model. For all test cases no efforts have been made to control mixing through the mixing time scale as is a common practice

JrnlID 10494_ArtID 9626_Proof#1 - 19/06/2015

and the same constant was used. Although it is well known that adjustments of the mixing constant C_ϕ could have led to more realistic degrees of extinction this would diminish the assessment of the predictive capabilities of the MMC-*enhanced* mixing models in terms of particle number dependence.

Acknowledgments Support is acknowledged from Deutsche Forschungsgemeinschaft (DFG) under grant number KR3684/7-1. Dr Vogiatzaki would like to acknowledge the contribution of The Lloyds Register Foundation. Lloyds Register Foundation helps to protect life and property by supporting engineering-related education, public engagement and the application of research.

References

1. Barlow, R., Frank, J.: Effects of turbulence on species mass fractions in methane/air jet flames. Proc. Combust Inst **27**, 1087–1095 (1998)
2. Barlow, R., Frank, J., Karpetis, A., Chen, J.Y.: Piloted methane/air jet flames: Transport effects and aspects of scalar structure. Combust. Flame **143**, 433–449 (2005)
3. Cao, R., Pope, S.: The influence of chemical mechanisms on pdf calculations of nonpremixed piloted jet flames. Combust. Flame **143**, 450–470 (2005)
4. Cao, R., Wang, H., Pope, S.: The effect of mixing models in pdf calculations of piloted jet flames. Proc. Combust Inst **31**, 15431550 (2007)
5. Chen, H., Chen, S., Kraichnan, R.: Probability distribution of a stochastically advected scalar field. Phys. Rev. Lett. **63**(24), 2657–60 (1989)
6. Sung, C.J., Law, C., Chen, J.: Augmented reduced mechanisms for no emission in methane oxidation. Combust. Flame **125**(1–2), 906–919 (2001)
7. Cleary, M., Kronenburg, A.: Hybrid multiple mapping conditioning on passive and reactive scalars. Combust. Flame **151**(4), 623–638 (2007)
8. Corrsin, S.: J. Aeronaut. Sci. **18**, 417 (1951)
9. Curl, R., Miller, R., Ralph, J., Towell, G.: Dispersed phase mixing: Ii. measurements in organic dispersed systems. AIChE J. **9**, 175–181 (1963)
10. Dopazo, C.: Probability density function approach for a turbulent heated jet. centerline evolution. Phys. Fluids **18**, 397–404 (1975)
11. Gardiner, C.: Handbook of stochastic methods. Springer, New York (1984)
12. Ge, Y., Cleary, M., Klimenko, A.: Sparse-lagrangian {FDF} simulations of sandia flame e with density coupling. Proc. Combust. Inst. **33**(1), 1401–1409 (2011)
13. Ge, Y., Cleary, M., Klimenko, A.: A comparative study of sandia flame series (df) using sparse-lagrangian {MMC} modelling. Proc. Combust. Inst. **34**(1), 1325–1332 (2013)
14. Haworth, D.: Progress in probability density function methods for turbulent reacting flows. Prog. Energy Combust. Sci. **36**, 168259 (2010)
15. He, G.W., Zhang, Z.F.: Two-point closure strategy in the mapping closure approximation approach. Phys. Rev. E **70**(036), 309 (2004)
16. Janicka, J., Kolbe, W., Kollmann, W.: Closure of the transport equation for the probability density function of turbulent scalar fields. J. Nonequil. Thermodyn **4**, 47–66 (1979)
17. Klimenko, A.: Modern modelling of turbulent non-premixed combustion and reaction of pollution emission. Proceedings of Clean Air VII, Lisbon, Portugal (2003)
18. Klimenko, A.: Matching the conditional variance as a criterion for selecting parameters in the simplest multiple mapping conditioning models. Phys. Fluids **16**(12), 4754–4757 (2004)
19. Klimenko, A.: On simulating scalar transport by mixing between lagrangian particles. Phys. Fluids **19**(3), 31,702 (2007)
20. Klimenko, A., Bilger, R.: Conditional moment closure for turbulent combustion. Prog. Energy Combust. Sci **25**(6), 595–687 (1999)
21. Klimenko, A., Pope, S.: The modeling of turbulent reactive flows based on multiple mapping conditioning. Phys. Fluids **15**(7), 1907–1925 (2003)
22. Kronenburg, A., Cleary, M.J.: Multiple mapping conditioning for flames with partial premixing. Combust. Flame **155**, 215–231 (2008)
23. Launder, B., Spalding, D.: The numerical computation of turbulent flows. Comput. Methods Appl. Mech. Eng. **3**(2), 269–289 (1974)

JrnlID 10494_ArtID 9626_Proof#1 - 19/06/2015

24. Lindstedt, R., Louloudi, S., Vaos, E.M.: Joint scalar probability density function modeling of pollutant formation in piloted turbulent jet diffusion flames with comprehensive chemistry. Proc. Combust Inst **28**(1), 149156 (2000)
25. Muradoglu, M., Jenny, P., Pope, S.B., Caughey, D.A.: A consistent hybrid finite-volume/particle method for the pdf equations of turbulent reactive flows. J. Comp. Phys. **154**, 342371 (1999)
26. Norris, A., Pope, S.: Turbulent mixing model based on ordering pairing. Combust. Flame **83**(1–2), 27–42 (1991)
27. Pope, S.: PDF methods for turbulent reactive flows. Prog. Energy Combust. Sci. **11**(2), 119–192 (1985)
28. Pope, S.: Mapping closures for turbulent mixing and reaction. Theor. Comput. Fluid Dyn **2**(5–6), 255–70 (1991)
29. Pope, S.B.: A model for turbulent mixing based on shadow-position conditioning. Phys. Fluids **25**(11) (2013)
30. Raman, V., Pitsch, H.: A consistent les/filtered-density function formulation for the simulation of turbulent flames with detailed chemistry. Proc Combust Inst **31**, 1711–1719 (2007)
31. Subramaniam, S., Pope, S.: A mixing model for turbulent reactive flows based on euclidean minimum spanning trees. Combust. Flame **115**(4), 487–514 (1999)
32. Vogiatzaki, K., Cleary, M., Kronenburg, A., Kent, J.: Modeling of scalar mixing in turbulent jet flames by multiple mapping conditioning. Phys. Fluids **21**(2) (2009)
33. Vogiatzaki, K., Kronenburg, A., Navarro-Martinez, S., Jones, W.: Stochastic multiple mapping conditioning for a piloted, turbulent jet diffusion flame. Proc. Combust Inst **33**(1), 1523–1531 (2011)
34. Wandel, A., Klimenko, A.: Testing multiple mapping conditioning mixing for monte carlo probability density function simulations. Phys. Fluids **17**(12), 128,105 (2005)
35. Wandel, A.P., Lindstedt, R.P.: Hybrid multiple mapping conditioning modeling of local extinction. Proc. Combust. Inst. **34**(1), 1365–1372 (2013)
36. Xu, J., Pope, S.B.: Pdf calculations of turbulent nonpremixed flames with local extinction. Combust. Flame **123**(3), 281–307 (2000)

AUTHOR QUERY

No Query.